

# OSCILLATION POWER AS A TEST OF STELLAR TURBULENCE : SCANNING THE HR DIAGRAM

Réza Samadi, M.-J. Goupil, Y. Lebreton, and A. Baglin

Observatoire de Paris-Meudon, 5 place Jules Janssen, F-92195 Meudon, France

## ABSTRACT

The acoustic power injected by turbulent convection into solar-like oscillations depends on the details of the turbulent spectrum. A theoretical formulation for the oscillation power is developed which generalizes previous ones. The formulation is first calibrated on a solar model in such a way as to reproduce the solar seismic data. This allows to investigate different assumptions about the stellar turbulent spectrum. We next explore consequences of the assumed turbulent description for some potentially solar-like oscillating stars. Large differences are found in the oscillation power of a given star when using different turbulent spectra as well as in a star to star comparison. Space seismic observations of such stars will be valuable for discriminating between several turbulent models.

## 1. INTRODUCTION

The acoustic power injected into the  $p$  modes by turbulent convection has been modeled by several authors (Balmforth, 1992; Goldreich et al., 1994; Goldreich & Keeley, 1977). In Samadi & Goupil (2000) a general formulation is proposed which allows to investigate more consistently different assumptions about the stellar turbulence such as its turbulent energy spectrum.

Providing that accurate measurements of the oscillation amplitudes and damping rates are available it is possible to evaluate the power injected into the modes and thus- by comparison with the observations- to constrain current theories (Samadi & Houdek, 2000).

In the present paper, the formulation, viewed as a diagnostic tool of stellar turbulent spectra, is used to compute oscillations power of several solar-like stars. We show that the expected low detection threshold of a space seismic experiment such as COROT (Baglin & The Corot Team, 1998) for instance will provide highly accurate acoustic power spectra and therefore important information on the associated turbulent

spectrum if the solar-like oscillating targets are properly chosen.

## 2. POWER INJECTED INTO SOLAR-LIKE OSCILLATIONS

### 2.1. Stochastic excitation

The acoustic power injected into the oscillations is defined (e.g. Goldreich et al., 1994) in terms of the damping rate  $\eta$ , the mean-square amplitude  $\langle A^2 \rangle$ , the mode inertia  $I$  and oscillation frequency  $\omega$  :

$$P(\omega) = \eta \langle A^2 \rangle I \omega^2 \quad (1)$$

The mean-square amplitude accounts for both the excitation by turbulent convection and the damping processes. It can be written in a simplified expression as

$$\langle A^2 \rangle \propto \eta^{-1} \int_0^M dm \rho_0 w^4 \left( \frac{\partial \xi_r}{\partial r} \right)^2 \mathcal{S}(\omega, m) \quad (2)$$

where  $\xi_r$  is the radial displacement eigenfunction,  $\rho_0$  the density,  $w$  the vertical rms velocity of the convective elements and  $\mathcal{S}$  the turbulent source function accounting for both the Reynolds and the entropy fluctuations. Detailed expressions for  $\langle A^2 \rangle$  and  $\mathcal{S}$  are given in Samadi & Goupil (2000). The source function involves the turbulent kinetic energy spectrum  $E(k)$  and the turbulent spectrum  $E_s(k)$  of the entropy fluctuations which can be related to  $E(k)$  (e.g. Samadi et al., 2000a). The turbulent spectra in  $\mathcal{S}$  are integrated over all eddy wavenumbers  $k$  and  $\mathcal{S}$  is in turn integrated in Eq.(2) over the stellar mass  $M$ .

### 2.2. Models for the solar turbulence

From the turbulence theory it is expected that  $E(k)$  follows the Kolmogorov spectrum as  $E(k) \propto k^p$  with the slope  $p = -5/3$ . Observations of the solar granulation allow one to determine the turbulent kinetic

spectrum  $E(k)$  of the Sun. Observations of the solar granulation by Espagnet et al. (1993) and Nesis et al. (1993). confirm the existence of a turbulent cascade with  $p \simeq -5/3$ . On the other hand, in the  $k$  range (small  $k$ ) prior to the turbulent cascade of slope  $p \simeq -5/3$ , Espagnet et al. (1993) determined a regime with a slope close to 0.7 whereas Nesis et al. (1993) found a slope of  $p = -5$ .

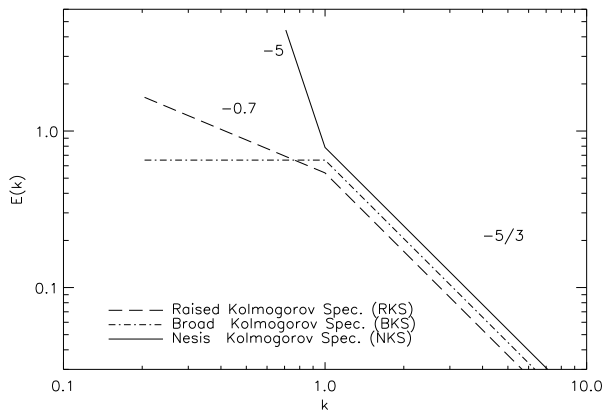


Figure 1. Kinetic turbulent spectra versus wavenumber  $k$ .

The spectrum observed by Espagnet et al. (1993) is modeled by the so called “Raised Kolmogorov Spectrum” (RKS hereafter) as suggested by Musielak et al. (1994). We also consider two additional spectra: the “Nesis Kolmogorov Spectrum” (NKS hereafter) - in agreement with the observations of Nesis et al. (1993) - and the “Broad Kolmogorov Spectrum” (BKS hereafter). These spectra (Figure 1) obey the Kolmogorov law for  $k \geq k_0$  where  $k_0$  is the wavenumber at which the turbulent cascade begins.

The wavenumber  $k_0$  is unknown but can be related to the mixing length  $\Lambda$  as  $k_0 = 2\pi / (\beta\Lambda)$  where  $\beta$  is a free parameter introduced for the arbitrariness of such definition (Samadi & Goupil, 2000). Moreover the definition of the eddy time correlation, which enters the description of the turbulent excitation, is somewhat arbitrary and is therefore gauged by introducing an additional free parameter  $\lambda$ . We show that the oscillation power computed on the Sun is very sensitive to the values of the free parameters  $\lambda$ ,  $\beta$  in Samadi et al. (2000a).

### 2.3. The solar case: comparison with observations and calibration of the free parameters

The power injected into the solar oscillations is related to the rms value  $v_s$  of the surface velocity as

$$v_s^2 = \xi_r^2(r_s) P / 2\eta I \quad (3)$$

where  $r_s$  is the radius at which oscillations are measured. Observations of the solar oscillations provide  $v_s$  and  $\eta$  such that  $P(\omega)$  can be evaluated according to Eq.(3).

The power  $P(\omega)$  is computed for a calibrated solar model obtained with the CESAM code (Morel, 1997). Convection is described according to the classical mixing-length theory (Böhm - Vitense, 1958). The oscillation properties were obtained from the adiabatic FILOU pulsation code of Tran Minh & Leon (1995). The physical ingredients of the model are detailed in Samadi & Houdek (2000).

The free parameters are then adjusted to obtain the best fit of the frequency dependence and the maximum amplitude to the solar observations by Libbrecht (1988).

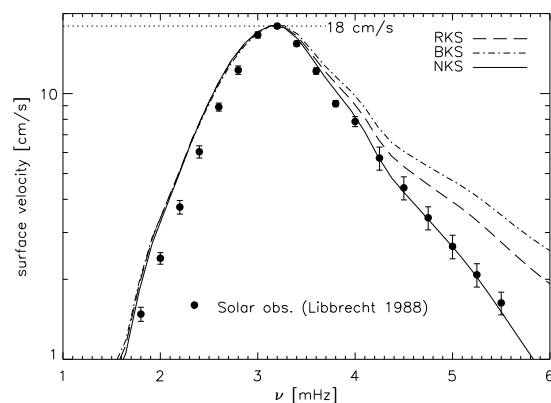


Figure 2. Computed surface velocity  $v_s$  (Eq.3) assuming the different turbulent spectra of Fig.(1).  $\lambda$  and  $\beta$  values result from fitting the computed  $v_s$  to the solar seismic observations by Libbrecht (1988) using the observed damping rate  $\eta$ .

Results of the fitting are shown in Fig. 2. All spectra of Fig 1 fit well the solar observations at low frequency ( $\nu \lesssim 3.5$  mHz) while the main differences are observed at high frequency. The overall best agreement is obtained with the NKS. Details of the resulting adjustments are given in Samadi et al. (2000a).

## 3. SCANNING THE HR DIAGRAM

### 3.1. The models

We focus on low intermediate mass stars ( $1 \lesssim M \lesssim 2M_\odot$ ) because the existence of an outer convective shell enables stochastic excitation. The thickness of the convective shell depends in particular on the star luminosity ( $L$ ) and effective temperature ( $T_{\text{eff}}$ ). We thus consider six models well distributed in the solar-like oscillation region (Table 1). These models are based on the fundamental parameters of several bright stars which were selected as targets for EVRIS (Baglin et al., 1993). The equilibrium models and the associated eigenfunctions of these stars are obtained in the same way as for the solar model.

Models		$L$ [ $L_{\odot}$ ]	$T_{\text{eff}}$ [K]	$M$ [ $M_{\odot}$ ]	$\nu_c$ [mHz]	Age [Gyr]
<i>A</i>	$\alpha$ Tri	12.1	6350	1.68	1.0	1.79
<i>B</i>	$\eta$ Boo	9.0	6050	1.44	1.0	3.05
<i>C</i>	Procyon	6.6	6400	1.46	1.5	2.40
<i>D</i>	$\beta$ Hyrdi	3.7	5740	1.08	1.5	7.33
<i>E</i>	$\beta$ Vir	3.5	6120	1.25	2.3	4.10
<i>F</i>	$\pi^3$ Ori	2.6	6420	1.25	3.6	1.76

Table 1. Stellar Parameters of selected stars.  $\nu_c$  is the cut-off frequency. For each model we have given the corresponding bright star from the EVRIS preliminary list of targets.

### 3.2. Star to star comparison

The acoustic power is computed for each selected star and for each of the three turbulent spectra of Fig.1 and is plotted for four of them in Fig.3. Of our 5 stars, model *E* is the closest to the Sun in the HR diagram (Figure 4), hence its structure (assuming here the same chemical composition) is nearly the same than in the solar case. Accordingly the oscillation spectrum of model *E* is quite similar to the solar one (except small differences at high frequency) and therefore does not show large differences when using different turbulent spectra (due to the solar calibration mentioned in Sect. 2.2); only small differences can be seen at high frequency. Same conclusion can be drawn for model *D*.

For a hotter star, the oscillation spectra computed with different turbulent spectra differ at low frequencies. As it is illustrated with the error bars and the detection threshold in Fig.2, such differences are significant enough to constrain stellar turbulent spectra providing that accurate measurements of  $P(\omega)$  are available.

Differences in oscillation power between model *E* (equivalently the Sun) and the other stars is related to the more extended outer convective zone (CZ hereafter) of model *E*. As the thickness of its CZ is larger, excitation of the low frequency oscillations involves all turbulent eddies. Therefore as for the Sun the power injected into low frequency oscillations is mainly governed by the eigenfunction behavior ( $\partial\xi_r/\partial r$  and I) and not by the behavior of the turbulence in the energy injection range (i.e at large turbulent scale).

For the other hotter stars, the relative smaller size of their CZ causes the excitation region to be localized in a thinner domain where changes in the properties of  $\xi_r$  are large. At a given frequency the extension of the excitation region changes with the considered turbulent spectra. Therefore the shape of  $P(\omega)$  is very sensitive to both the properties of  $\xi_r$  - thus to  $\omega$  - and the behavior of the turbulent spectra. As a result, significantly large differences in term of  $P(\omega)$  are observed when using different turbulent spectra. This feature is also well explained for Procyon (model *C*) in Samadi et al. (2000b).

Besides a temperature effect, there is also a luminosity (or mass) effect although much smaller. This is illustrated with model *F* which is much hotter than model *E* but shows only a very weak sensitivity to the choice of the turbulent spectrum when computing  $P(\omega)$  (not shown here). In that sense, model *F* is closer to the cooler model *E* than to the other stars with similar effective temperatures. It is an intermediate case as it is less massive than for instance model *C*. Therefore the excitation region for this star extends deeper down compared to that of Procyon (model *C*).

Figure 4 presents a star to star comparison of the oscillation power computed assuming the NKS. The plot is performed in the HR diagram in order to depict the dependence of the power spectrum  $P(\omega)$  with the effective temperature and the luminosity. As the star becomes hotter and more luminous the frequency domain where  $P(\omega)$  takes significant values becomes smaller. This is due to the decrease of the cut-off frequency with increasing values of  $T_{\text{eff}}$  and  $L$ .

### 3.3. Observational constraints

Observations of solar-like oscillations in Procyon have yet been only clearly discovered by Martic et al. (1999) and Barban et al. (1999) in spectroscopic surface velocity measurements. However currently Butler & et al. (2000) claimed the detection of solar like oscillations in  $\beta$  Hydri.

Most of the current ground based observations are mainly limited by the daily aliases. In particular they cannot yet provide the growth rates  $\eta$  which are necessary in order to compute  $P(\omega)$  from Eq.(1). Thus we need observations of solar-like oscillations performed in such a way as to avoid the daily aliases. In particular space based experiments are particularly adapted for asteroseismology. The forthcoming space project COROT (Baglin & the Corot team, 1998) based on photometric measurements will reach a noise level of 0.7 ppm (Auvergne & the COROT Team, 2000) and will thus detect oscillation amplitudes comparable to the solar ones ( $\sim 2$  ppm). Furthermore the instrument will continuously monitor several stars during  $\sim 150$  days giving a frequency precision of  $\sim 0.1 \mu\text{Hz}$  such that accurate measurements of  $\eta$  will be available.

Will this high accuracy enable us to constrain the theory of the stochastic excitation and the stellar turbulence? The answer depends on the detection threshold and the accuracy in term of  $P(\omega)$ . For our stars here,  $\eta$  are not currently available. It is possible however to evaluate crudely a detection threshold for  $P(\omega)$ . Indeed, the power is related to the root mean-square of the surface velocity  $v_s$  according to Eq.(3) where  $r_s$  is set to the radius at which  $T = T_{\text{eff}}$ . In the adiabatic assumption  $v_s$  is in turn simply related to the luminosity fluctuation  $\delta L$  approximatively as

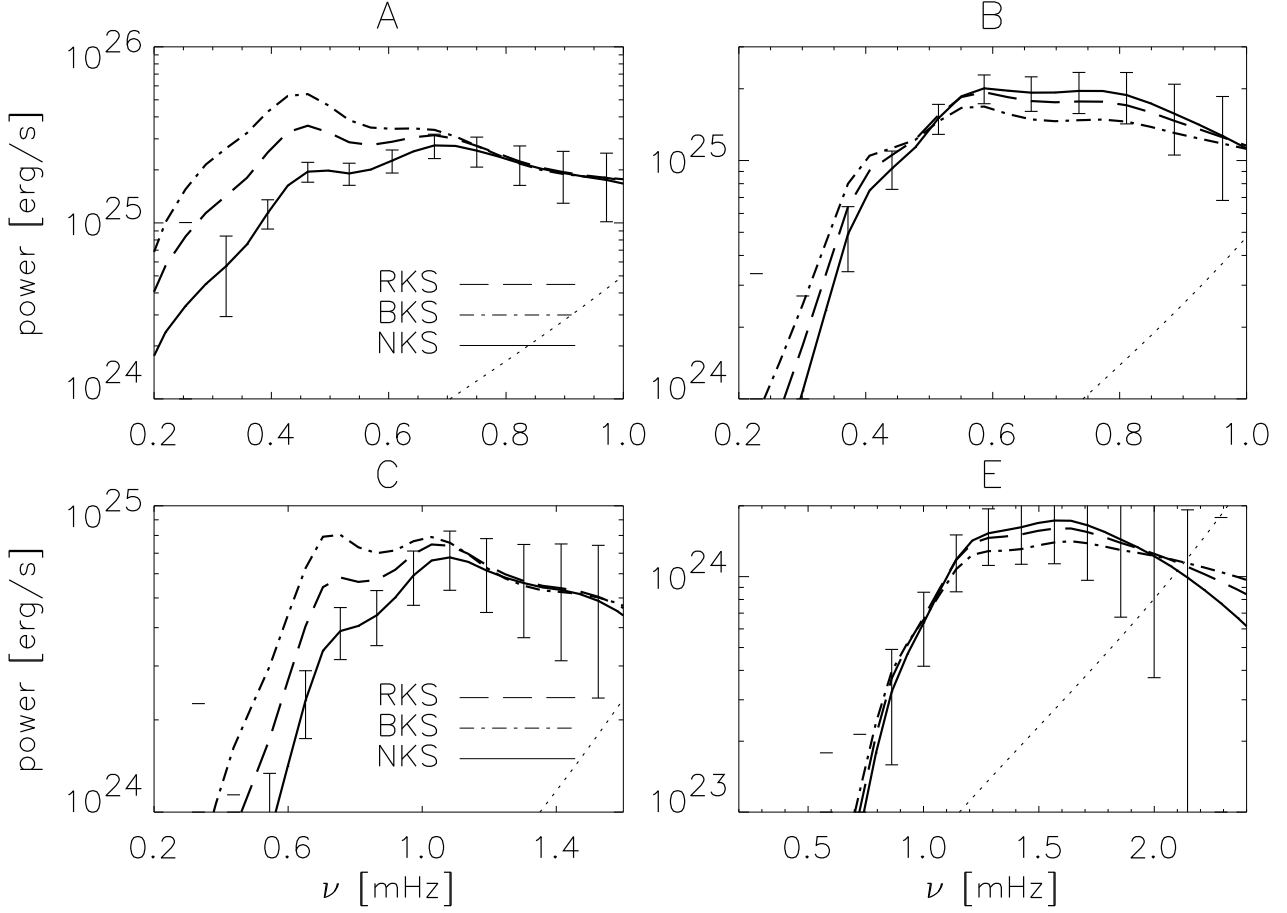


Figure 3. Oscillation power  $P$  versus frequency ( $\nu = \omega/2\pi$ ) assuming the different spectra of Fig.1 for the stars : A, B, C and E. Vertical error bars  $\Delta P$  (plotted on the solid line) were obtained from Eq.(8) assuming an accuracy for  $\eta/2\pi$  (resp.  $\delta L/L$ ) of  $0.1 \mu\text{Hz}$  (resp.  $0.7 \text{ ppm}$ ). For each star the detection threshold calculated according to Eq.(7) is represented by a dotted line.

(Kjeldsen & Bedding, 1995)

$$\delta L/L \propto v_s T_{\text{eff}}^{-1/2} \quad (4)$$

Eq.(3) and Eq.(4) enable us to derive an approximate relation

$$\frac{P}{P_{\odot}} \approx \left( \frac{\delta L/L}{\delta L_{\odot}/L_{\odot}} \right)^2 \frac{T_{\text{eff}} \eta I \xi_r^{-2}}{(T_{\text{eff}} \eta I \xi_r^{-2})_{\odot}} \quad (5)$$

where quantities with a  $\odot$  are relative to the Sun. Goldreich & Kumar (1991) derived a simplified equation for  $\eta$  which allows us to express  $\eta/\eta_{\odot}$  as (see Houdek, 1996, section 3.4.4)

$$\frac{\eta}{\eta_{\odot}} = \frac{L (H c_s^{-2} \omega R)^2 I^{-1}}{L_{\odot} (H c_s^{-2} \omega R)_{\odot}^2 I_{\odot}^{-1}} \quad (6)$$

where  $c_s$  and  $H$  are the sound speed and the pressure scale height respectively evaluated at the top of the convection zone and  $R$  is the star radius. Let  $s$  be the detection threshold in terms of relative luminosity fluctuation  $\delta L/L$  expressed in unity of  $(\delta L/L)_{\odot}$ . The detection threshold  $P^{\text{th}}(\omega)$  in terms of oscillation power can be expressed with the help of Eqs(5,6)

as

$$P^{\text{th}}(\omega) = b s^2 P_{\odot}^{\text{max}} \frac{R^2 \xi_r^{-2}(\omega) \omega^2}{R_{\odot}^2 \xi_{r,\odot}^{-2}(\omega_{\text{max}}) \omega_{\text{max}}^2} \quad (7)$$

$$\text{with } b = T_{\text{eff}} L H^2 c_s^{-4} / (T_{\text{eff}} L H^2 c_s^{-4})_{\odot}$$

where  $\omega_{\text{max}}$  and  $P_{\odot}^{\text{max}}$  are the frequency position and the power at the maximum value of  $\delta L_{\odot}/L_{\odot}$ . In addition from Eq.(6) relative error bar in term of  $P$  can be expressed as

$$\frac{\Delta P}{P} = 2 \frac{\Delta \delta L}{\delta L} + \frac{\Delta \eta}{\eta} \quad (8)$$

where  $\eta$  and  $\delta L$  are evaluated according to Eqs.(6,5).

In Fig.3 the detection threshold  $P^{\text{th}}(\omega)$  is plotted for the case  $s = 1$  which corresponds to 3 times the noise level (rms) of the COROT instrument. In addition the error bars  $\Delta P$  according to Eq.(8) is plotted assuming COROT's performances, *i.e.*  $\Delta \eta/2\pi \sim 0.1 \mu\text{Hz}$  and  $\Delta \delta L \sim 0.7 \text{ ppm}$ . Note that, as for the Sun,  $\Delta P$  is larger at high and low frequency because  $\delta L$  becomes very smaller.

We conclude that the differences between the spectra for the hotter stars (models A and C) are sufficiently

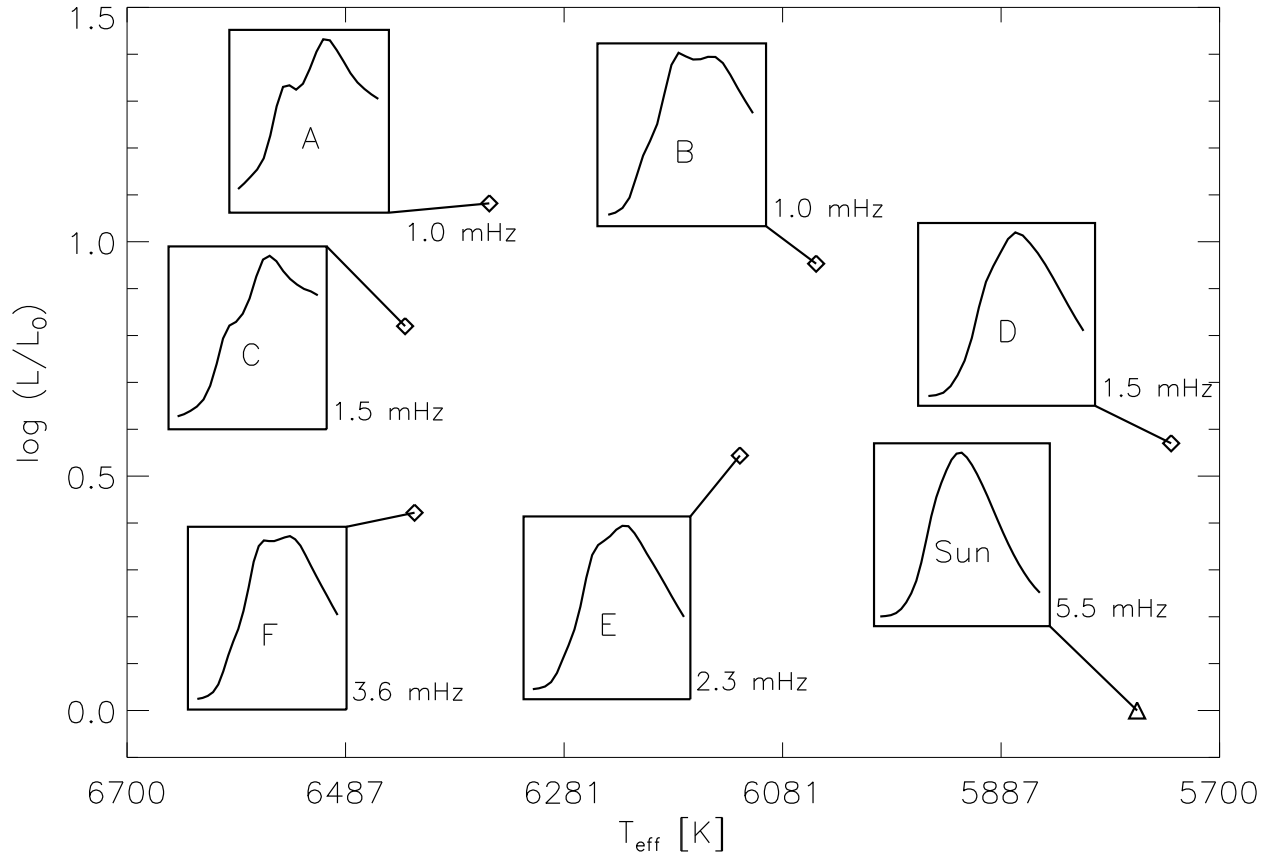


Figure 4. Positions of the selected stars in the HR diagram (filled squared). For each star the computed power spectrum assuming the NKS is shown in an associated box. Abscissa extend from 0 to the acoustic cut off frequency : the frequency range of the oscillation power narrows for more massive stars.

large compared to error bars to identify the best turbulent spectrum.

## CONCLUSION

This work shows that for stars hotter and more massive than the Sun, the formulation of the power  $P(\omega)$  injected into the solar-like oscillations is very sensitive to the way the turbulent stellar spectrum is modeled. For the Sun it is presently possible to constrain the solar turbulent spectrum from observations of the granulation. Such information is not directly available for other stars. Evaluation of  $P(\omega)$  derived from the seismic observations of the solar-like oscillations (amplitudes and damping rates) will therefore provide constraints on the stellar turbulence.

In addition for a given spectrum it is found that the shape of  $P(\omega)$  versus  $\omega$  can change quite significantly from one star to the other. These differences are related to the size of the convection zone which depends on the fundamental parameters of the stars. A star to star comparison of the power derived from observations will thus provide additional constraints.

The accuracy of an observational determination of  $P(\omega)$  depends on the accuracy of the measurements of the associated oscillation fluctuations  $\delta L$  and the oscillations damping rates  $\eta$ . A crude relation derived in the present work allows to evaluate the COROT detection threshold and the accuracy in terms of  $P(\omega)$ . It suggests that futur space observations of such solar-like oscillating stars will measure acoustic powers  $P(\omega)$  with an accuracy which will able us to identify the turbulent spectrum closest to reality.

## REFERENCES

- Auvergne M., the COROT Team, april 2000, In: The Third MONS Workshop : Science Preparation and Target Selection, 135–138
- Baglin A., The Corot Team, 1998, In: IAU Symp. 185: New Eyes to See Inside the Sun and Stars, vol. 185, 301
- Baglin A., Weiss W., Bisnovatyi-Kogan G., 1993, In: Baglin A., W. Weiss W. (eds.) Inside the stars, 756
- Balmforth N.J., Apr. 1992, MNRAS, 255, 639

- Barban C., Michel E., Martic M., et al., Oct. 1999, A&A, 350, 617
- Böhm - Vitense E., 1958, Zeitschr. Astrophys., 46, 108
- Butler P., et al., 2000, (in preparation)
- Espagnet O., Muller R., Roudier T., Mein N., Apr. 1993, A&A, 271, 589
- Goldreich P., Keeley D.A., Feb. 1977, ApJ, 212, 243
- Goldreich P., Kumar P., jun 1991, ApJ, 374, 366
- Goldreich P., Murray N., Kumar P., Mar. 1994, ApJ, 424, 466
- Houdek G., 1996, Pulsation of Solar-type Stars, Ph.D. thesis, Institut für Astronomie , Wien
- Kjeldsen H., Bedding T.R., Jan. 1995, A&A, 293, 87
- Libbrecht K.G., Nov. 1988, ApJ, 334, 510
- Martic M., Schmitt J., Lebrun J.C., et al., 1999, A&A, 351, 993
- Morel P., Sep. 1997, A&AS, 124, 597
- Musielak Z.E., Rosner R., Stein R.F., Ulmschneider P., Mar. 1994, ApJ, 423, 474
- Nesis A., Hanslmeier A., Hammer R., et al., Nov. 1993, A&A, 279, 599
- Samadi R., Goupil M.J., 2000, A&A(submitted)
- Samadi R., Houdek G., april 2000, In: The Third MONS Workshop : Science Preparation and Target Selection, 27–32
- Samadi R., Goupil M.J., Lebreton Y., 2000a, A&A(submitted)
- Samadi R., Houdek G., Goupil M.J., Lebreton Y., 2000b, in preparation
- Tran Minh F., Leon L., 1995, In: Physical Process in Astrophysics, 219